ABSOLUTE NEUTRON CROSS SECTIONS FOR THE PRODUCTION OF ^{24}Na ISOMER FROM MAGNESIUM AND ALUMINUM

FINAL REPORT

October, 1970

NATIONAL AERONAUTICS AND SPACE ADMINISTRATION

MULTIDISCIPLINARY GRANT NGL 44-007-006

SMU NO. 83-24

GEORGE N. SALAITA
Department of Physics

SOUTHERN METHODIST UNIVERSITY

DALLAS, TEXAS 75222

Absolute Neutron Cross Sections for the Production of ^{24}Na Isomer from Magnesium and Aluminum

George N. Salaita
Department of Physics, Southern Methodist University
Dallas, Texas 75222

Abstract: The cross sections for the $^{24}Mg(n,p)^{24m}Na$ and $^{27}Al(n,\alpha)^{24m}Na$ reactions were measured using the cyclic activation technique and a high energy resolution Ge(Li) gamma-ray detector. The absolute activation cross sections have also been measured for the $^{27}Al(n,p)^{27}Mg$ and $^{27}Al(n,\alpha)^{24}Na$ reactions at 14.8 MeV neutron energy. The results were: $^{24}Mg(n,p)^{24m}Na$, 138 ± 14 mb; $^{27}Al(n,\alpha)^{24m}Na$, 65 ± 6 mb; $^{27}Al(n,p)^{27}Mg$, 75 ± 6 mb; and $^{27}Al(n,\alpha)^{24}Na$, 111 ± 9 mb. These results are compared with similar measurements of other authors.

E

RADIOACTIVITY ^{24m}Na [from Mg(n,p), Al(n,α)]; measured $T_{1/2}$, γ-spectrum, σ.

NUCLEAR REACTIONS ^{27}Al(n,α), ^{27}Al(n,p), E = 14.8 ± 0.3 MeV; measured σ.

Natural targets.

1. Introduction

This investigation is concerned with the measurement of the absolute cross sections for two 14-MeV neutron reactions, $^{24}Mg(n,p)^{24m}Na$ and $^{27}Al(n,\alpha)^{24m}Na$, which give rise to the same product, the 20 ms (millisecond) half-life ^{24}Na isomeric state. This isomer was identified[1] through study of the decay of ^{24}Ne which leads by beta emission to the residual nucleus ^{24}Na. Subsequently, several workers[2-8] reported measurements of the transition energy, the half-life, and the production cross sections of the ^{24}Na isomer via the (n,p) and (n,α) reactions in magnesium and aluminum, respectively. The values of the cross sections reported by different authors differ from each other by a factor of two or more for the same reaction[2,5,8].

In an earlier publication Salaita et al.[9] reported the value of the ratio of isotopic ^{24}Mg to the ^{27}Al cross sections for the production of isomeric ^{24}Na to be 2.05 ± 0.14.

The present work is a sequal to the previous one and was undertaken with the objective of measuring accurately the production cross sections of ^{24}Na isomer in magnesium and aluminum. In the present investigation, advantages are gained from the utilization of the cyclic (repetitive) activation method and the use of a high energy resolution Ge(Li) gamma-ray detector. A further objective was to study the feasibility of employing the cyclic activation technique for elemental analysis by measuring short-lived isomeric activities between successive fast neutron bursts.

2. Experimental Arrangement and Procedure

2.1 Apparatus

The pulsed neutron source consisted of a 400 - kv Van de Graaff accelerator fitted with a deflecting plates assembly. The assembly was placed at a position immediately before the beam analyzing magnet. This position was chosen so as to have the deflected beam strike a water-cooled beam catcher as far away from the tritium target as was conveniently possible. The plates were positioned in vertical planes so that the beam was deflected horizontally in a large target room. Combinations of burst lengths from 1 to 10^5 μsec (duty cycle not to exceed 90%) and repetition rates from 1 to 10^5 pps were available. The rise and decay times on the burst were better than 0.5 μsec. The burst of deuteron beam current was monitored by observing with an oscilloscope the voltage produced by an emitter-follower circuit. Neutrons of about 15-MeV energy were obtained from the $T(d,n)^4He$ reaction using magnetically analyzed incident deuteron beams of 300 keV energy. The air-cooled titanium tritide target was at one end of a "Y" tube made of stainless steel, the other branch of the "Y" contained an alpha detector. The neutron yield was measured by the associated particle technique, detecting alpha particles at 168° to the deuteron beam by a silicon surface barrier, Si(Li) detector. The target, scattering sample, and gamma-ray detector were located in a large room.

Figure 1 shows the geometric arrangement for observing gamma rays

produced from neutron activation of the samples. The scattering samples of aluminum and magnesium were machined from pure metals in shape of rings. These rings had an inside diameter of 3.25-in and an outside diameter of 5.25-in. The axial thickness of the rings was 0.7-in. The sample was mounted on the detector housing with its axis in the direction of the deuteron beam, and its center at a distance of 9.3-in from the center of the target. As a result of this geometry, the neutrons were incident on the ring at an average angle of 7° with respect to the beam.

The gamma-ray detector was a planar lithium-drifted germanium, Ge(Li) 6.4 cm^2 x 7.5 mm - 17pF. The energy resolution (FWHM) of the detector system was 2.8 keV for the 1332.52 keV ^{60}Co gamma line. Energy calibration of the spectrometer was made daily by using one or more known energy gamma rays from ^{137}Cs, ^{60}Co, ^{22}Na, ^{65}Zn, and ^{7}Be standard sources. The detector was shielded from the direct neutron beam by a tungsten cone 6.5-in long.

The gamma-ray pulses from the detector were amplified by a TENNELEC TC-200 amplifier, shaped by a TC-611 baseline restorer, and then recorded with a Nuclear Data 1024-channel pulse-height analyzer with an Analog to Digital Converter (ADC) of 4096 conversion gain address full scale. A schematic block diagram of electronics and experimental arrangement is depicted in Figure 2.

To obtain the cross sections for the productions of ^{24}Na isomer via the reactions $^{24}Mg(n,p)^{24m}Na$ and $^{27}Al(n,\alpha)^{24m}Na$ one must know the

number of atoms available for the particular reaction, the gamma-ray yield from the decay of the isomeric state to the ground state of ^{24}Na, and the neutron flux incident on the scattering sample. These points are considered in detail in the following sections.

2.2 Cyclic Activation

Short-lived isomeric activities produced in a nuclear reaction may be studied by bombarding the target material with particles from a pulsed machine and recording the gamma-ray spectrum in the time interval between beam pulses. The ^{24}Na isomeric activity under investigation has a half-life of 20 ms and can be conveniently measured during the short time interval between successive bursts of a pulsed neutron source. This method was described by Hickman and Hegedüs[10] and by Givens et al.[11] The technique is primarily based on the principle of irradiating the sample with a relatively short burst of fast neutrons, introducing a sufficient time delay before data recording, then counting of the activation gamma-ray spectrum before the next burst. This process is repetitive and thus the name "cyclic" is adapted. The activity which would be produced by a series of pulses as a function of pulse width, period between pulses, delay and counting intervals can be optemized by a proper choice of these parameters. Consider the timing diagram depicted in Figure 3 which illustrates a bombard-wait-count cycle with arbitrary bombard, wait,

and count periods of duration t_b, t_d, and t_c respectively, and which is repeated with a period $T \geq t_b + t_d + t_c$. The activity which is produced due to a particular reaction, from a neutron burst can be expressed as

$$A_1 = N\phi\sigma(1 - e^{-\lambda t_b}) \tag{1}$$

and the activity at the end of the first delay period t_d is

$$A_{11} = N\phi\sigma(1 - e^{-\lambda t_b})e^{-\lambda t_d} \tag{2}$$

The detector response (number of counts) measured after the first burst during t_c is

$$D_1 = A_{11}\varepsilon \frac{1 - e^{-\lambda t_c}}{\lambda} \tag{3}$$

While the detector response after the n^{th} pulse during t_c is

$$D_n = D_1(1 + e^{-\lambda T} + e^{-2\lambda T} + \ldots + e^{-(n-1)\lambda T}) \tag{4}$$

$$= \frac{N\phi\sigma\varepsilon}{\lambda}(1 - e^{-\lambda t_b})(e^{-\lambda t_d})(1 - e^{-\lambda t_c})\frac{(1 - e^{-n\lambda T})}{(1 - e^{-\lambda T})}$$

where the sum of the terms

$$(1 + e^{-\lambda T} + e^{-2\lambda T} + \ldots + e^{-(n-1)\lambda T}) = \frac{(1 - e^{-n\lambda T})}{(1 - e^{-\lambda T})}$$

has been substituted in (4).

The cumulative detector response after time t(= nT) is obtained by summing the responses from all counting intervals and is easily seen to be

$$D_t = \frac{N\phi\sigma\varepsilon}{\lambda} (1 - e^{-\lambda t_b})(e^{-\lambda t_d})(1 - e^{-\lambda t_c}) \times \left[\frac{n}{(1 - e^{-\lambda T})} - \frac{e^{-\lambda T}(1 - e^{-n\lambda T})}{(1 - e^{-\lambda T})^2} \right] \quad (5)$$

where

N = number of nuclei available for a given reaction,

ϕ = neutron flux (neutrons/cm^2·sec) during a burst,

σ = reaction cross section (cm^2),

ε = efficiency of the detector for the gamma rays observed in the ring geometry,

λ = decay constant of the radioactivity produced (sec^{-1}),

t_b = neutron burst width (sec),

t_d = time delay between the end of a neutron burst and beginning of counting interval (sec),

t_c = counting interval (sec),

T = the period of repetition of bursts (sec), and

t = nT = elapsed clocktime (sec).

The scattering samples were irradiated for a total experiment time which ranged from 2 to 5 hours and the desired activity determined from the photopeak area and the corresponding detector efficiency.

2.3 Method of Efficiency Determination

The absolute detection efficiency of the Ge(Li) detector for the ring geometry were experimentally determined using calibrated radioactive isotopes as gamma-ray sources. The calibrated sources were solutions of ^{7}Be(477.56 keV, ±4%), ^{65}Zn(1115.52 keV, ±4%), ^{60}Co(1173.23 and 1332.52 keV, ±4%) and ^{24}Na(1368.57 and 2753.92 keV, ±8%) in thin-wall toroidal containers having the same dimensions as the scattering rings. The containers were machined of plexiglass in order to reduce gamma-ray absorption. An aliquot of suitable strength was withdrawn from the standard solution diluted and placed in one of the toroids. Water was then added to fill the entire volume of the toroid. This was placed around the detector in the same geometry as the acti-

vation measurements and the particular photopeak counting rate was determined. The results of the measurements for the absolute photopeak efficiency as a function of gamma-ray energy is shown in Figure 4. As is seen from the figure, the logarithm of the photopeak efficiency ε is a linear function of the logarith of the gamma-ray energy E_γ for energies between about 500 and 1332.52 keV. Since our present concern is primarily measuring gamma rays less than 1500 keV, two least-squares fits were obtained; one was based on the first four efficiency data points and the other on the above four and the point for the 2753.92 keV photopeak from ^{24}Na. The relations obtained by a least-squares fit were

$$\ell n(10^4\varepsilon) = 4.966 - (1.267)\ell nE_\gamma$$

and (6)

$$\ell n(10^4\varepsilon) = 4.815 - (1.215)\ell nE_\gamma$$

for four and five data points, respectively. The root-mean-square deviations of the experimental points from a linear least-squares fit are 1.1% for the four points and 1.4% for the five points. The reason for the large deviation in the latter case can be attributed to the large uncertainty (8%) in the ^{24}Na standard. The variations of the photopeak efficiency as a function of the axial position of

the source was measured for two standards in order to correct for possible positioning error. A maximum change of 6% in the efficiency was observed when the axial position was varied by 5 mm. In this experiment the scattering rings could be placed symmetrically to an accuracy of better than 1 mm and therefore no appreciable error would arise in this way.

The gamma-ray absorption in aluminum for the ^{7}Be photopeak (477.56 keV) was experimentally deduced by taking the ratio of the photopeak counts from two toroids containing equal amounts of the standard. One container was filled with water and the other with pure aluminum grains. Water was added to the latter until the entire gap was filled. The self-absorption factor was also calculated from the expression[12,13]:

$$K = \int_{r_1}^{r_2} e^{-\mu(r - r_1)} \frac{dr}{r} \Big/ \int_{r_1}^{r_2} \frac{dr}{r} \qquad (7)$$

where μ is the total linear absorption coefficient of gamma rays in the sample material and r_1 and r_2 are the inner and outer radii of the ring sample, respectively. The calculated value was slightly smaller than the experimental value. The effect of the self-absorption was calculated using Equation (7).

2.4 Neutron Flux Measurements

During the course of the activation measurements, the neutron was continuously monitored by the associated particle technique, detecting alpha particles at 168° to the deuteron beam using a silicon surface barrier detector. In order to relate the alpha rate and neutron yield and for the purpose of calculating the flux at the position of the scattering rings, high-purity (99.9%) copper disks were activated, and the neutron flux in the 14-MeV energy region was determined in accordance with the Texas Convention[14]. The foils were placed at the position of the scattering samples and at several other locations with respect to the direction of the deuteron beam. The induced activity of the samples was determined from the photopeak of the annihilation radiation detected, using a 3-in × 3-in NaI(Tℓ) scintillation spectrometer. The results of the measurements showed that the flux as calculated from the alpha monitor is in good agreement with that measured by the copper foils, when the latter are placed forward along a line joining the alpha monitor to the target. For positions other than along this line or about 10° on either side of it, the results show a large difference between the values of the neutron flux thus obtained. This difference may be attributed to the variation of the (d,t) neutron intensity with angle and to the variation of copper-63 reaction cross section with neutron energy. The effect of the tungsten cone on the fast

neutron flux at the scattering ring was investigated by activating foils with the cone in position and with it removed. No significant change was detected in the induced activity per monitor count.

2.5 Multiple Scattering

A factor related to the problem of flux measurement is that of neutron multiple scattering in the sample. The probability of a neutron being scattered more than once is dependent on the dimensions of the scatterer and the scattering cross section. Day[15] has shown that if the radial and axial thickness of the ring do not differ by more than a factor of two, the effects of multiple scattering cancel out the neutron attenuation at the first collision. One can, to a good approximation, assume that the neutron flux is constant throughout the scatterer. The validity of this assumption was checked by Nishimura et al.[13] and found to be applicable within the experimental error. Since the scattering rings of this work have dimensions whose ratio (10 to 7) fall within the prescribed factor, the above approximation was assumed to apply in the present measurements.

3. Cross Section Measurements

Since the present work was primarily concerned with the determination of the absolute value of the production cross sections

for the 20 ms half-life ^{24}Na isomeric activity in magnesium and aluminum by the (n,p) and (n,α) reactions, respectively, it was considered advisable and worthwhile to measure the ^{27}Al(n,p)^{27}Mg and ^{27}Al(n,α)^{24}Na cross sections at 14.8 ± 0.3 MeV neutrons.

In a recent compilation of the (n,p) cross sections for approximately 14 MeV neutrons, Gardner[16] pointed out several serious discrepancies among values reported by different authors. In particular, sixteen measurements of the (n,p) cross section in aluminum have been reported, and these range from 52 ± 10 to 87 ± 7 to 140 ± 30 mb. The reported maximum and minimum limits are 170 and 42 mb.

Many investigators have measured the neutron cross section for the (n,α) reaction in aluminum in the vicinity of 14 MeV. The average value of the cross section at 14.5 MeV is about 116 mb. In general, the agreement between the various reported values of the cross section for this reaction is good to within 5%. The agreement between experimental values and theoretical calculations is also good[17,18,19].

3.1 (n,p) Reaction in Aluminum

This reaction in the isotope ^{27}Al leads to the residual nucleus ^{27}Mg which decays with a half-life of 9.46 minutes to various levels of ^{27}Al. A 69% branch (β^-) goes to the 843.71 keV level and 31%

to the 1014.49 keV level in ^{27}Al. The 1014.49 keV level decays with 97% probability to the ground state and with 3% probability to the first excited state.

To measure the (n,p) cross section the ring sample was irradiated for 45 minutes and one minute after the end of irradiation it was placed around the Ge(Li) detector and counted for 30 minutes. After each measurement the back ground count was recorded and found to be negligible. The gamma-ray spectrum obtained from this reaction is shown in Figure 5. The energy of the photopeaks was measured by activating two one-gallon can size blocks of aluminum and recording the spectrum simultaneously with standard sources of ^{137}Cs and ^{60}Co.

The initial activity was determined from the areas under the 843.71 and 1014.49 keV photopeaks. The cross section at 14.8 ± .3 MeV was calculated from the relation:

$$\sigma = \frac{\lambda N_p \, e^{\lambda t_d} \, (1 - e^{-\lambda t_c})^{-1} \, (1 - e^{-\lambda t_b})^{-1}}{\phi N b \varepsilon K} \qquad (8)$$

where N_p is the photopeak area, b is the number of gamma rays per disintegration, K is the absorption correction of the gamma rays produced in the sample, and the remaining symbols are as defined in Equation (5). The absolute cross section for the (n,p) reaction

in Aluminum is given in Table 1. This value is the average of several determinations.

3.2 (n,α) Reaction in Aluminum

This reaction in ^{27}Al leads to the residual nucleua ^{24}Na which is beta active decaying to the various levels of ^{24}Mg. The ground state of ^{24}Na decays mainly (99.92%) to the 4122.54 keV level of ^{24}Mg which de-excites by gamma emission to the 1368.57 keV level. The latter level decays by gamma emission to the ground state of ^{24}Mg.

The aluminum ring sample was irradiated for a duration of six to eight hours, after which the sample was counted for a period of three hours. Varying delay times from the end of irradiation were introduced for the purpose of allowing short-lived activities to decay before the ^{24}Na activity was counted. For the purpose of half-life determination, the activity of the 1368.57 keV photopeak was followed for several half-lives. The measured half-life was found to be 14.98 ± 0.02 hours. The gamma-ray spectrum obtained from this reaction is shown in Figure 6. In this figure the upper portion (1368.57 keV photopeak) was recorded approximately four and one-half hours prior to the lower portion. The induced activity was determined by measuring the area under

the 1368.57 keV photopeak after background correction. The cross section was then calculated from Equation (8) above.

3.3 ^{24}Na Isomer

The reaction $^{24}Mg(n,p)^{24}Na$ and $^{27}Al(n,\alpha)^{24}Na$ lead to the residual nucleus ^{24}Na which has an isomeric state 472.48 keV above the ground state. This activity can be recorded in the time interval between successive neutron bursts. In order to obtain maximum detector response for cyclic activation analysis, proper selection of the parameters in Equation (5) was necessary. It can easily be seen that the detector response is maximum for a given decay constant λ, a period T, and a run time nT, when $t_d = 0$ and $t_b = t_c = T/2$. However, it is experimentally advisable that short delays be introduced at the end of the burst before counting and prior to the next burst. Such delay will reduce the possibility of counting prompt radiations due to the neutron inelastic scattering at the expense of an acceptable decrease in the detector response.

For the present investigation a near maximum detector response was obtained by a timing combination of (20, 22, 20, 50), i.e., the fast neutron burst had a duration of 20 ms, the delay after the time zero pulse was 22 ms, following which the analyzer was gated on (coincidence) for 20 ms, and that the time zero pulses were separated by a period of 50 ms. The magnesium and aluminum rings

were irradiated for about 4.2×10^{11} and 4.8×10^{11} total neutrons per run, respectively. The gamma-ray spectra obtained are shown in Figures 7 and 8.

In addition to the 472.48 keV gamma ray from the ^{24}Na isomeric activity, 197.96 keV and 511 keV gamma rays were also produced. These peaks, which are present in the background spectra, were shown to be due to the interaction of scattered neutrons in the detector and its housing[20]. Figure 7 shows a very weak 350.89 keV gamma-ray line from the $^{24}Mg(n,\alpha)^{21}Ne$ reaction. The analyzed-beam current pulse was continuously monitored at the target with an oscilloscope. It was observed that occasionally the neutron burst width would stretch out to overlap momentarily the analyzer coincidence gate. This resulted in the detection of the above prompt radiation produced from the (n,α) reaction in magnesium.

3.4 Background and Errors

In many cases the limitation on the cross section accuracy that is obtainable is due to the presence of background peaks in the gamma-ray spectrum. Therefore, in order to determine the gamma-ray yield accurately, background sources must be properly subtracted.

The background contribution to the (n,p) and (n,α) reactions

in aluminum was insignificant. These spectra were recorded after a period of delay from the end of irradiation during which time the accelerator was turned off.

In the case of the cyclic activation of magnesium and aluminum a carbon ring was used as scatterer for background runs. The carbon ring has the same dimensions as the metal samples. Figure 9 shows typical background spectra obtained when no scatterer and when a carbon scatterer is used. The photopeaks in the spectra are produced by neutron interactions in the room, and with the detector and its housing system. The neutrons producing this background may be the room returned neutrons, but another source is the ring scatterer itself. The contribution of this latter source to the intensity of the 197.96 keV and 511 keV gammas is approximately 20 and 50%, respectively. Thus, the spectrum taken with carbon ring represents the background effects.

The principle errors in the measurement of the activation cross sections reported here arise in the determination of the gamma-ray yield and the neutron flux. The determination of the gamma-ray yield involves the photopeak counts, the photopeak efficiency, internal conversion correction, and a correction for the self-absorption in the scattering ring. The magnitude of the combined error in these quantities is about 7 to 8%. The standard

error in the measurement of the neutron flux in the experiment described here is believed to be about 4 to 5%. The errors in the remaining quantities entering Equations (5) and (8) are kept to a minimum since sample position and timing cycle have been measured with an accuracy better than 1%. An additional error is introduced in the cross section by the neutron multiple scattering which is estimated to be about 2%. These uncertainties, when combined quadratically, give values which vary from 8 to 10%. In the cyclic activation experiment the problem of background subtraction introduces an additional error of about 2%.

4. Results and Discussion

The measured activation cross sections at 14.8 ± 0.3 MeV neutron energy for the $^{27}Al(n,p)^{27}Mg$, and $^{27}Al(n,\alpha)^{24}Na$ were 75 ± 6 mb and 111 ± 9 mb, respectively. The experimental results, together with those of other authors, are listed in Table I. As is evident in this table, the agreement between the present results and recently reported values is, in general, rather good in this energy region.

The measured $^{27}Al(n,\alpha)^{24m}Na$ cross section is higher than previous measurements - being 8% higher than the closest previous measurement, that of Monnand[5], 60% higher than reported by Glagolev et al.[2], and 100% higher than measured by Van Zelst

et al.[8]

The $^{24}Mg(n,p)^{24m}Na$ is also higher than reported by the above investigators. The results, together with other measurements of the gamma-ray energy, the half-life of the isomeric activity, and the cross sections are presented in Table II. The ratio of the magnesium to the aluminum isomeric state production cross sections is in excellent agreement with the reported relative value.[9] The absolute cross sections were calculated from the isomeric activity by determining the area under the 472.48 keV photopeak after background subtraction. The background spectrum taken with the carbon ring was subtracted from each of the original spectra, Figures 7 and 8, after normalization to the same alpha monitor counts.

Since the 20 ms half life ^{24}Na isomeric activity is produced in both Mg and Al, this points out to the possibility of analysis for magnesium in the presence of aluminum in samples such as Basalt which contains approximately equal amounts[11] of Mg and Al. For in addition to 472.48 keV gamma ray from the ^{24}Na isomer, Al leads to the 9.46 min ^{27}Mg activity by the $^{27}Al(n,p)^{27}Mg$ reaction. Thus, it appears that if the 843.71 and 1014.49 keV gamma rays from the residual ^{27}Mg are produced in sufficient intensity during the cyclic activation run, they could provide a basis for Al analysis. As an exploratory study, Al blocks

were activated by the cyclic method until the 472.48 keV gamma ray was built up to a reasonable intensity. Three mintues after the end of the cyclic activation run the 843.71 and 1014.49 keV gammas were counted for 20 minutes. The resulting gamma-ray spectrum showed that the above two photopeaks were produced in a reasonable intensity relative to the 472.48 keV photopeak. This particular measurement does not constitute a realistic test for Al analysis, since it was obtained under ideal conditions. Additional studies under normal conditions are desirable.

References

1. B. J. Dropesky and A. W. Schardt, Phys. Rev., 102, 426 (1956).

2. V. L. Glagolev et al., Soviet Physics JETP, 36, 742 (1959).

3. G. S. Mani et al., Nucl. Phys., 19, 535 (1960).

4. V. L. Galgolev and P. A. Yampolskii, Soviet Physics JETP, 13, 528 (1961).

5. Edouard Monnand, "Etude de Corps Radioactifs a Vie Tres Breve Produito par Neutrons Rapids", CEA-R2900 (Centre d'Etudes Nucleaires de Grenoble, Decembre 1965).

6. P. Meyers and J. J. C. Schats, Physica, 32, 179 (1966).

7. B. A. Benetskii et al., Soviet Physics JETP, 18, 640 (1964).

8. L. Van Zelst, P. Meyers, and J. A. Oosting, Physica, 39, 463 (1968).

9. G. N. Salaita et al., Trans. Nucl. Sci. Eng., 11, 21 (1968).

10. G. D. Hickman and F. Hegedüs, Nucl. Inst. Meth., 32, 77 (1965).

11. W. W. Givens, W. R. Mills, and R. L. Caldwell, Nucl. Inst. Meth., 80, 95 (1970).

12. D. M. Van Potter et al., Phys. Rev., 128, 1246 (1962).

13. K. Nishimura et al., Nucl. Phys., 70, 421 (1965).

14. Proceedings of the 1965 International Conference on Modern Trends in Activation Analysis, April 19-22, 388, Texas A&M University.

15. R. B. Day, Phys. Rev., 102, 767 (1956).

16. D. G. Gardner, Nucl. Phys., 29, 373 (1962).

17. J. P. Butler and D. C. Santry, Can. J. Phys., 41, 372 (1963).

18. D. Crumpton et al., J. Inorg. Nucl. Chem., 31, 1 (1969).

19. R. C. Barrall, M. Silbergeld, and D. G. Gardner, Nucl. Phys., A 138, 387 (1969).

20. K. Przewlocki, G. N. Salaita, W. R. Mills, and W. W. Givens, "High Resolution Gamma-Ray Spectroscopy for Well Logging", Laboratory Memorandum No. 21, 1968, Mobil Research and Development Corp., Field Research Laboratory, Dallas, Texas.

21. M. J. Depraz, G. Legros, and M. R. Salin, J. Phys. Radium, 21, 377 (1960).

22. H. W. Schmitt and J. Halperin, Phys. Rev., 121, 827 (1961).

23. F. Gabbard and B. D. Kern, Phys. Rev., 128, 1276 (1962).

24. A. Paulsen and H. Liskien, J. Nucl. Energy parts A/B, 19, 907 (1965).

25. J. Lebowitz et al., IL Nuovo Cimento, LXV A, No. 4, 675 (1970).

26. A. Poularikas and R. W. Fink, Phys. Rev., 115, 989 (1959).

27. S. K. Mukherjee et al., Proc. Phys. Soc., LXXVII, No. 2, 508 (1961).

28. F. L. Hassler and R. A. Peck, Jr., Phys. Rev., 125, 1011 (1962).

29. G. C. Bonazzola et al., Nucl. Phys., 51, 337 (1964).

30. P. N. Tiwari and E. Kondaiah, Phys. Rev., 167, 1091 (1968); P. N. Tiwari and E. Kondaiah, Nucl. Phys., A 110, 317 (1968).

31. P. Cuzzocrea and E. Perillo, IL Nuovo Cimento, LIV B, No. 1, 53 (1968).

Acknowledgments

The author wishes to express his appreciation to Drs. W. R. Mills and W. W. Givens, and to Professor C. W. Tittle for helpful discussions, to M. Gill, P. K. Eapen, and R. Zombola for assistance in the data-taking. Thanks are due to Miss Ivanka Vavrin for typing the manuscript.

This research was sponsored by NASA under contract No. NGR-44-007-006.

List of Tables

TABLE I

Neutron Reaction Cross Sections in Aluminum

Reference	E_n(MeV)	Cross section (mb)
	$^{27}Al(n,\alpha)^{24}Na$	
Mani et al.[3] (1960)	14.75	113 ± 3
Depraz et al.[21] (1960)	15.0 ± 0.4	116 ± 9
Schmitt & Halperin[22] (1961)	14.76 ± 0.06	117 ± 8
Gabbard & Kern[23] (1962)	14.9	112 ± 11
Butler and Santry[17] (1963)	14.5 ± 0.06	116 ± 4
Paulsen & Liskien[24] (1965)	14.71 ± 0.27	119 ± 7
Crumpton et al.[18] (1969)	14.8	121 ± 6
Barrall et al.[19] (1969)	14.8 ± 0.2	116 ± 8
Lebowitz et al.[25] (1970)	14.7	110 ± 20
Present Work	14.8 ± 0.3	111 ± 9
	$^{27}Al(n,p)^{27}Mg$	
Poularikas & Fink[26] (1959)	14.8	53 ± 6
Mani et al.[3] (1960)	14.75	68 ± 5
Mukherjee et al.[27] (1961)	14.8	77 ± 7.7
Gabbard & Kern[23] (1962)	14.4	50 ± 7
Hassler & Peck[28] (1962)	14.4	93 ± 10
Bonazzola et al.[29] (1964)	14.7	66 ± 2
Tiwari & Kondaiah[30] (1968)	14.2	71 ± 9
Cuzzocrea & Perillo[31] (1968)	14.67 ± 0.09	78 ± 5
Present Work	14.8 ± 0.3	75 ± 6

TABLE II

Summary of Present and Other Cross Section Measurements for the Production of ^{24}Na Isomer

Reference	Target	Reaction	Energy (kev)	$T_{1/2}$ (ms)	Cross Section (mb)
Dropesky and Schardt[1]	Ne (gas)	$^{22}Ne(t,p)^{24}Ne$ $^{24}Ne(\beta^-)^{24}Na$	472 ± 4		
Glagolev et al.[2]	Al Mg	$^{27}Al(n,\alpha)^{24m}Na$ $^{24}Mg(n,p)^{24m}Na$	470 ± 10 470 ± 10	20 ± 1 20 ± 1	40 80
Mani et al.[3]	Al	$^{27}Al(n,\alpha)^{24m}Na$	472	25	
Glagolev and Yampolskii[4]	Al	$^{27}Al(n,\alpha)^{24m}Na$	470 ± 10	18.3 ± 0.6	
Monnand[5]	Al Mg	$^{27}Al(n,\alpha)^{24m}Na$ $^{24}Mg(n,p)^{24m}Na$	475 475	20 ± 0.6 20 ± 0.6	60 100
Meyers and Schats[6]	Al	$^{27}Al(n,\alpha)^{24m}Na$	470 ± 10	20 ± 0.7	
Benetskii et al.[7]	Mg	$^{24}Mg(n,p)^{24m}Na$	470	20	
Van Zelst et al.[8]	Al Mg	$^{27}Al(n,\alpha)^{24m}Na$ $^{24}Mg(n,p)^{24m}Na$			33 ± 10 48 ± 15
Present Work	Al Mg	$^{27}Al(n,\alpha)^{24m}Na$ $^{24}Mg(n,p)^{24m}Na$	472.48 472.48	20 ± 1	65 ± 6 138 ± 14

Figure Captions

Fig. 1. Experimental geometry for the present investigations.

Fig. 2. Experimental geometry and electronics block diagram.

Fig. 3. Representation of pulsing and counting time intervals.

Fig. 4. Photopeak efficiency of a Ge(Li) detector 6.4 cm^2 × 7.5 mm for ring geometry.

Fig. 5. Gamma-ray spectrum from ^{27}Mg obtained by irradiating an aluminum ring with 14.8 MeV neutrons.

Fig. 6. Gamma-ray spectrum from the $^{27}Al(n,\alpha)^{24}Na$ reaction. The upper and lower portions of the spectra were recorded by introducing 256- and 2048- channels digital zero shifts in the ADC, respectively.

Fig. 7. Low energy cyclic activation gamma-ray spectrum from Mg ring. The 350.89 keV photopeak is attributed to the prompt radiation from the $^{24}Mg(n,\alpha)^{21}Ne$ reaction.

Fig. 8. Low energy cyclic activation gamma-ray spectrum from Al ring. The 197.96 keV photopeak is from the detector system.

Fig. 9. Low energy background spectra. The upper curve (closed circles) was obtained with a carbon ring. The lower curve was obtained with no scatterer.

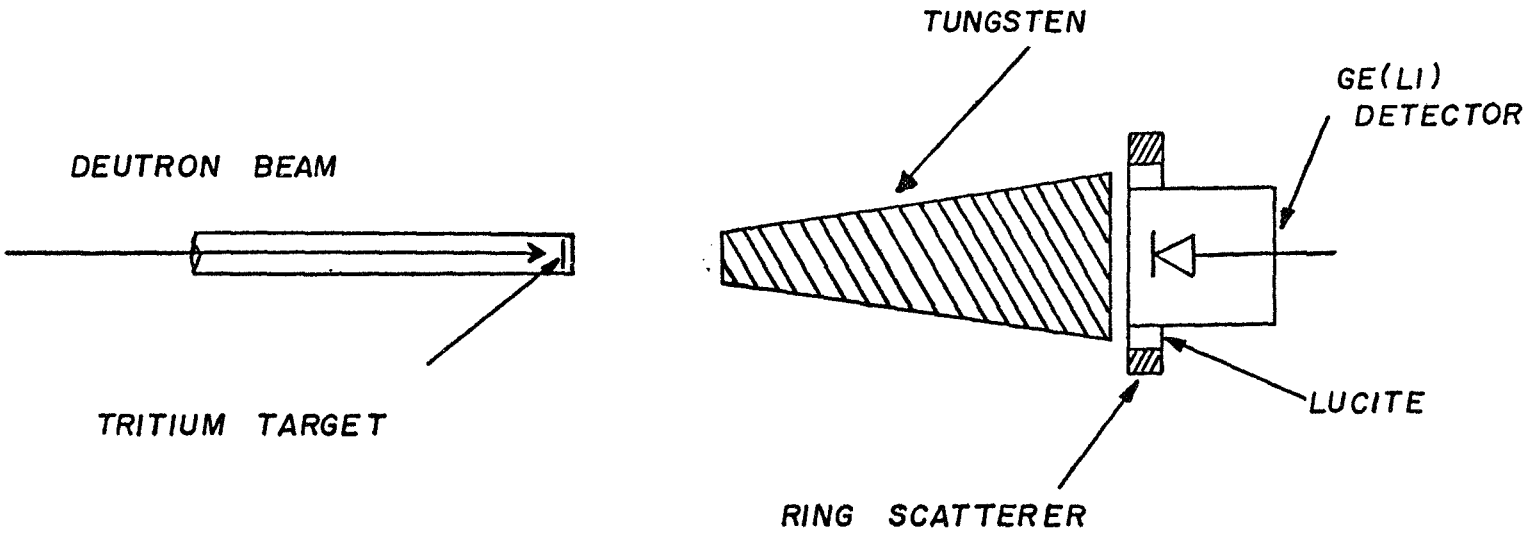
TUNGSTEN
GE(LI)
DETECTOR
DEUTRON BEAM
TRITIUM TARGET
LUCITE
RING SCATTERER

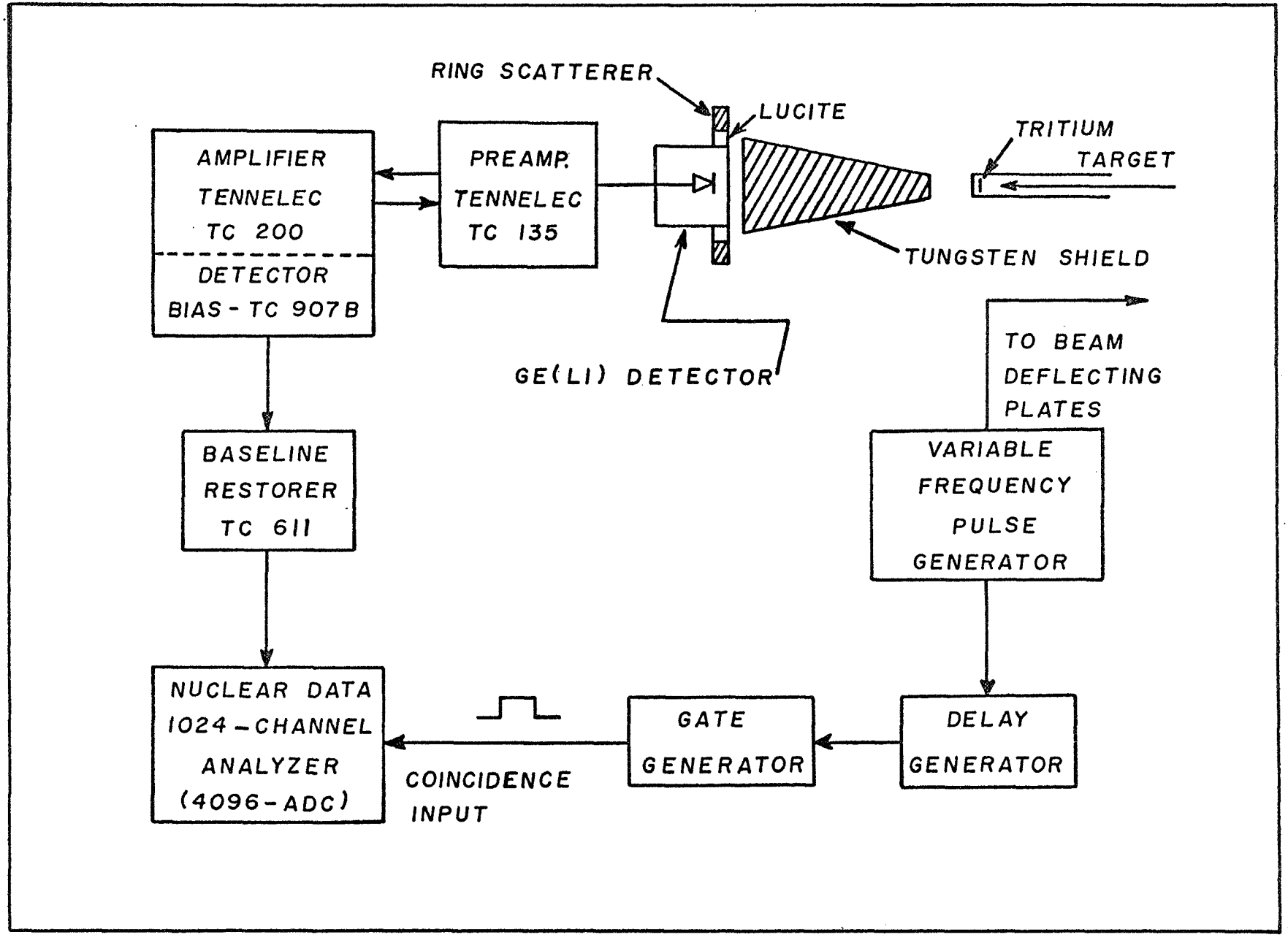
RING SCATTERER
LUCITE
TRITIUM
TARGET
AMPLIFIER
TENNELEC
TC 200
DETECTOR
BIAS - TC 907B
PREAMP.
TENNELEC
TC 135
TUNGSTEN SHIELD
GE(LI) DETECTOR
TO BEAM
DEFLECTING
PLATES
BASELINE
RESTORER
TC 611
VARIABLE
FREQUENCY
PULSE
GENERATOR
NUCLEAR DATA
1024-CHANNEL
ANALYZER
(4096-ADC)
COINCIDENCE
INPUT
GATE
GENERATOR
DELAY
GENERATOR

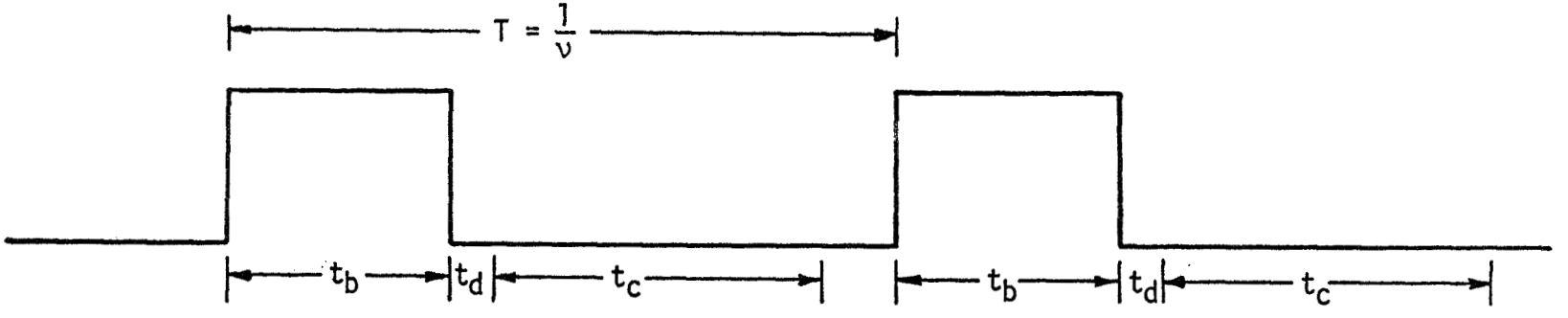
T = 1/ν
t_b
t_d
t_c
t_b
t_d
t_c

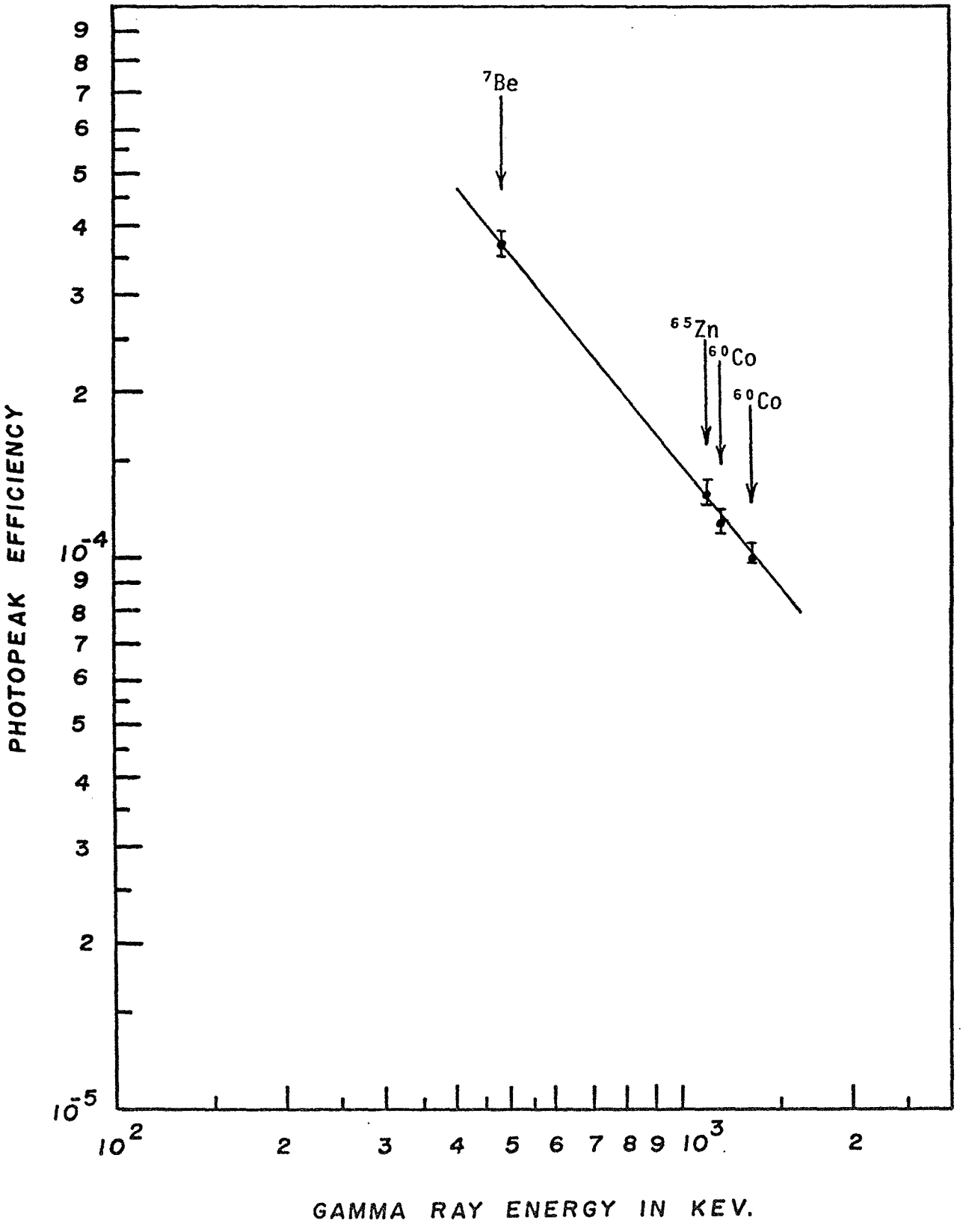
PHOTOPEAK EFFICIENCY
9
8
7
6
5
4
3
2
10^-4
9
8
7
6
5
4
3
2
10^-5
7Be
65Zn
60Co
60Co
10^2
2
3
4
5
6
7
8
9
10^3
2
GAMMA RAY ENERGY IN KEV.

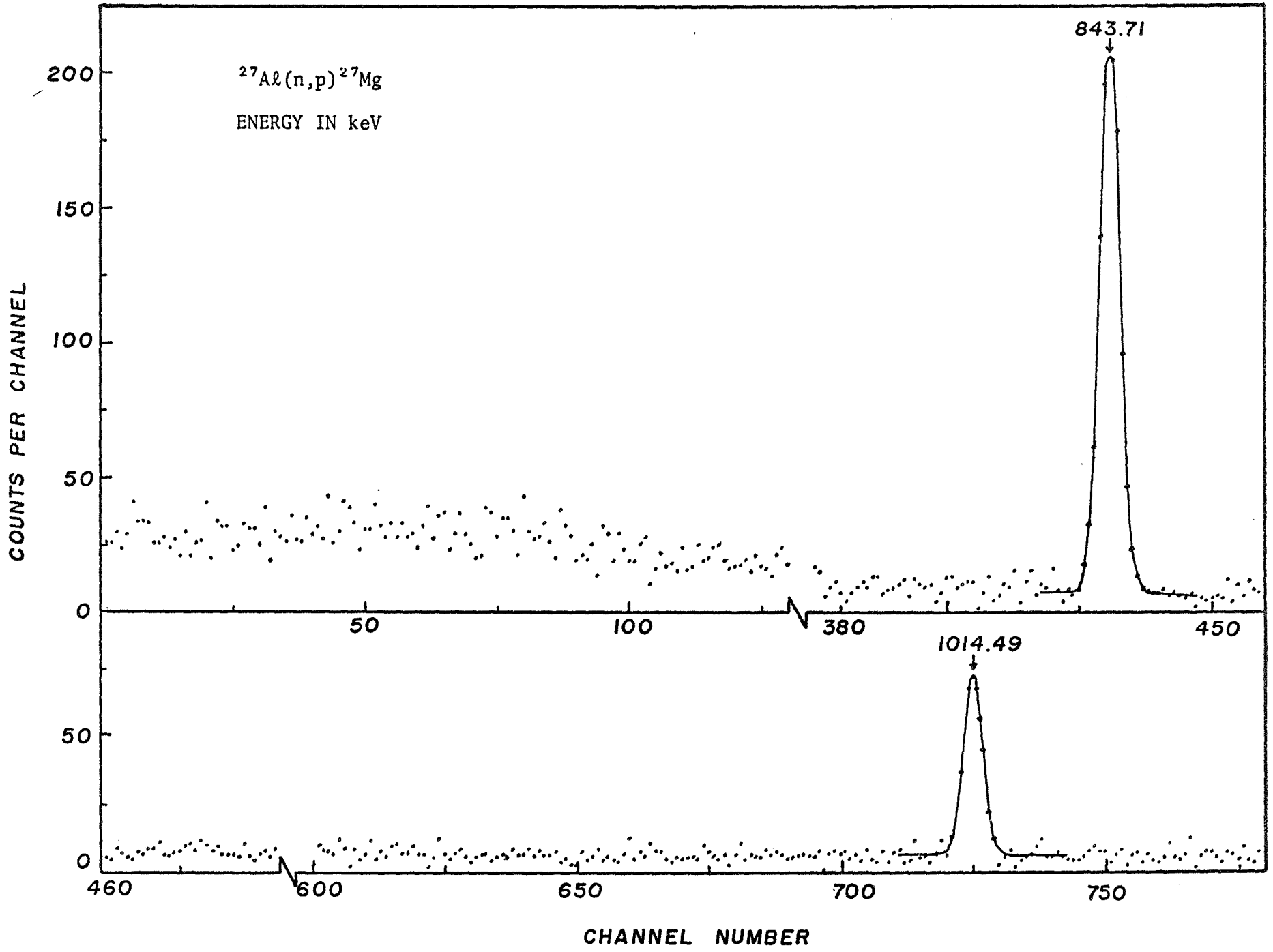
^{27}Aℓ(n,p)^{27}Mg
ENERGY IN keV
843.71
1014.49
COUNTS PER CHANNEL
CHANNEL NUMBER
200
150
100
50
0
50
100
380
450
50
0
460
600
650
700
750

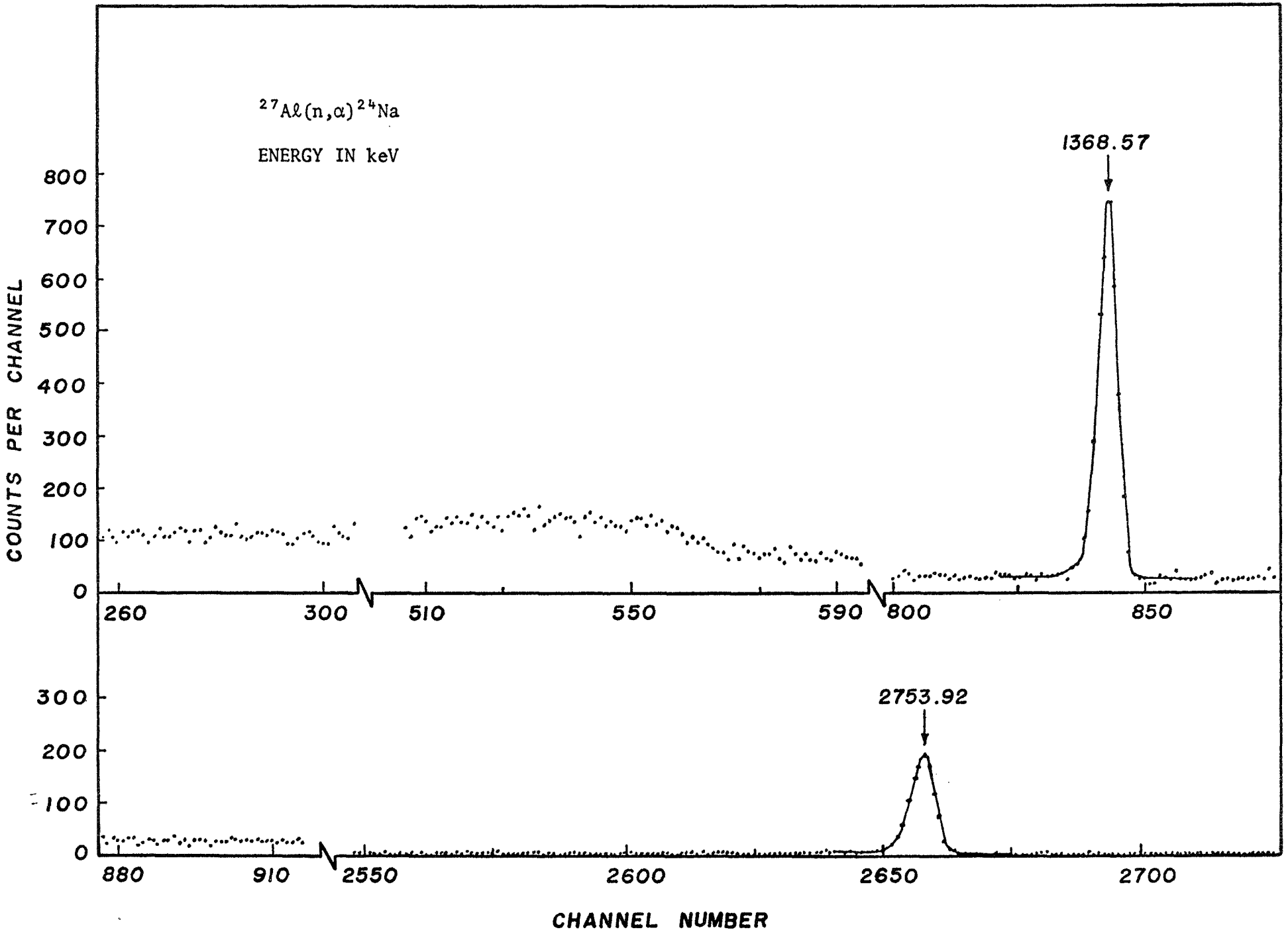
$^{27}Al(n,\alpha)^{24}Na$
ENERGY IN keV
1368.57
2753.92
COUNTS PER CHANNEL
CHANNEL NUMBER
0
100
200
300
400
500
600
700
800
260
300
510
550
590
800
850
880
910
2550
2600
2650
2700

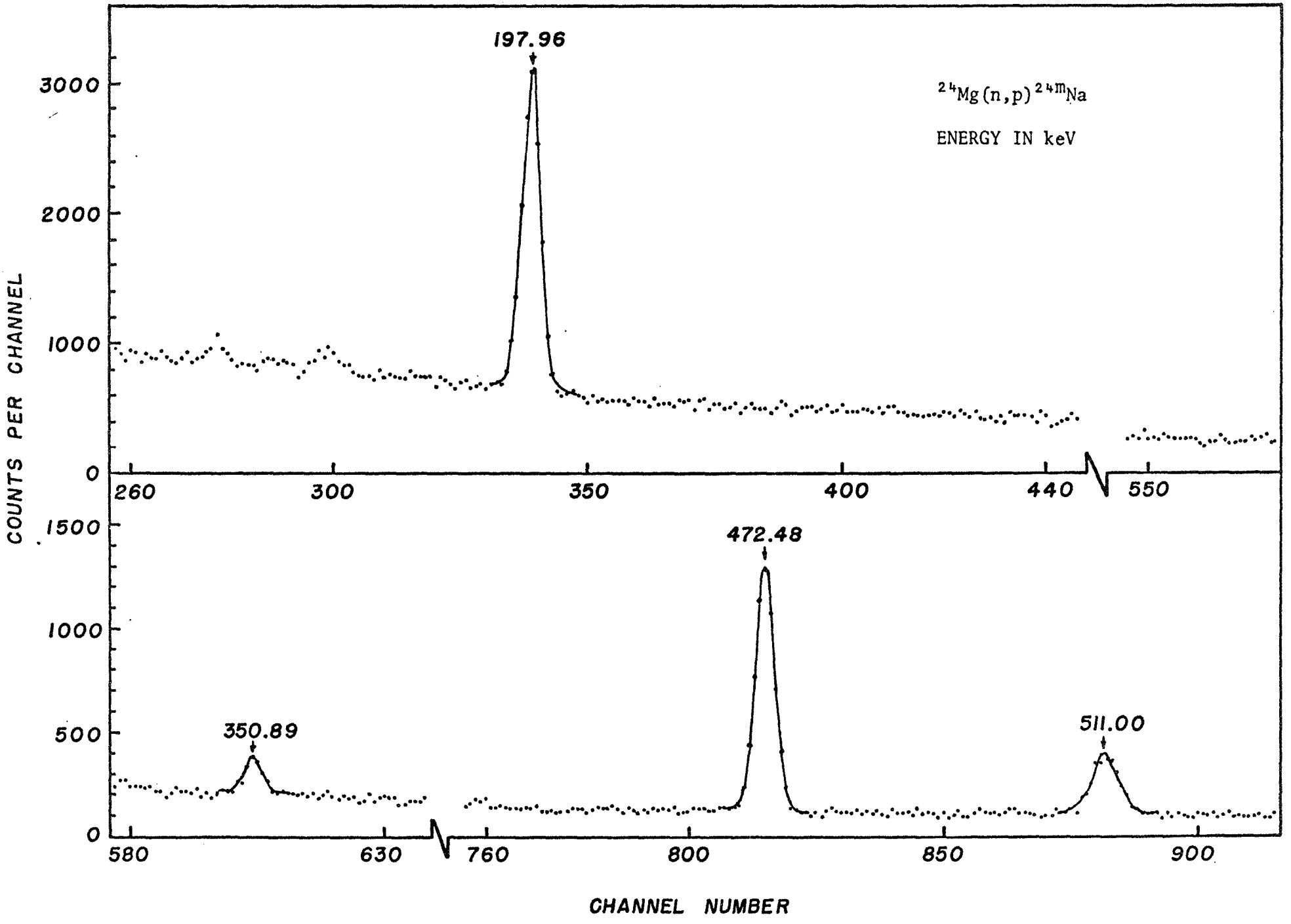
197.96
$^{24}Mg(n,p)^{24m}Na$
ENERGY IN keV
3000
2000
1000
0
260
300
350
400
440
550
472.48
1500
1000
500
0
350.89
511.00
580
630
760
800
850
900
COUNTS PER CHANNEL
CHANNEL NUMBER

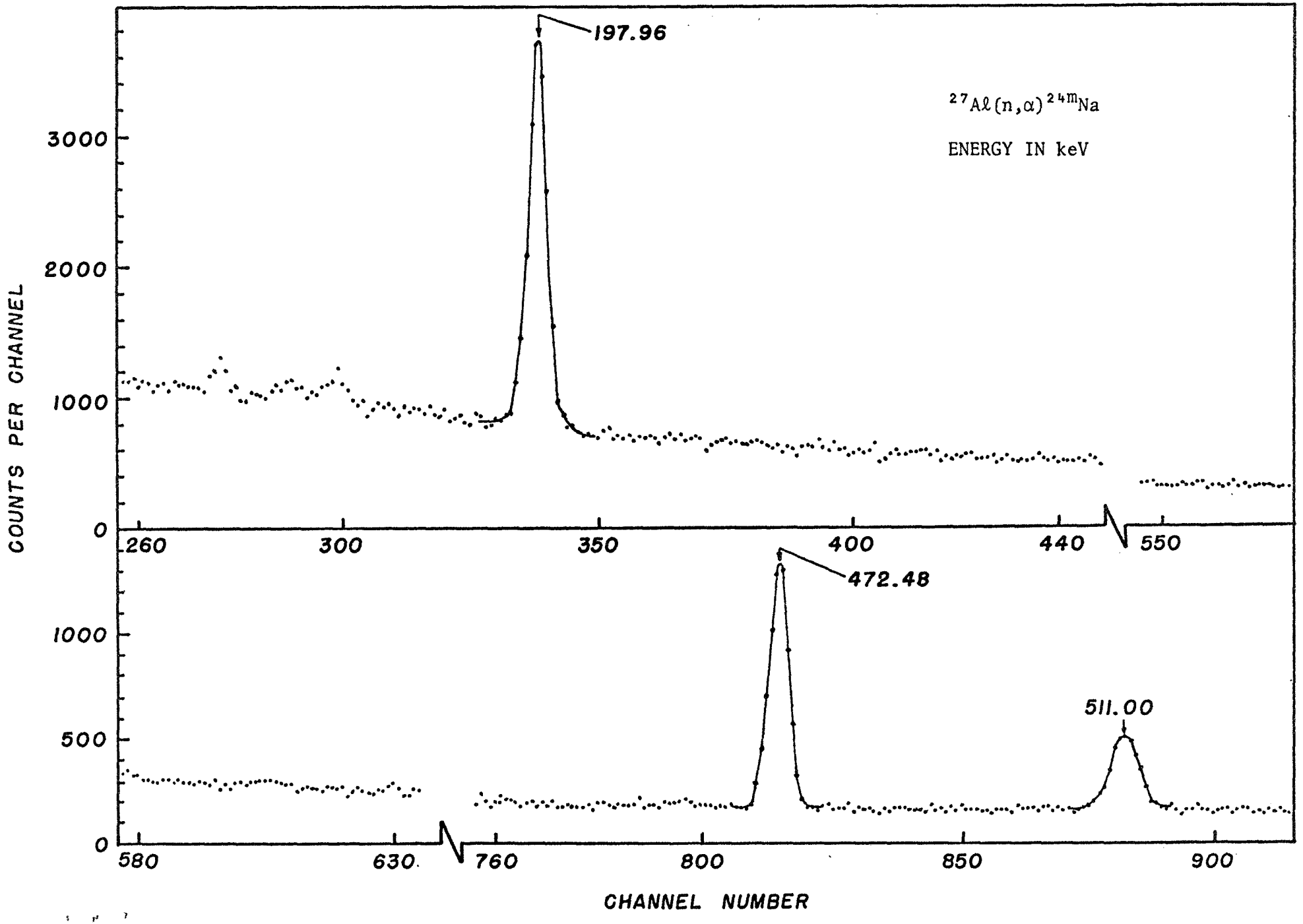
197.96
$^{27}Al(n,\alpha)^{24m}Na$
ENERGY IN keV
3000
2000
1000
0
260
300
350
400
440
550
472.48
511.00
1000
500
0
580
630
760
800
850
900
COUNTS PER CHANNEL
CHANNEL NUMBER

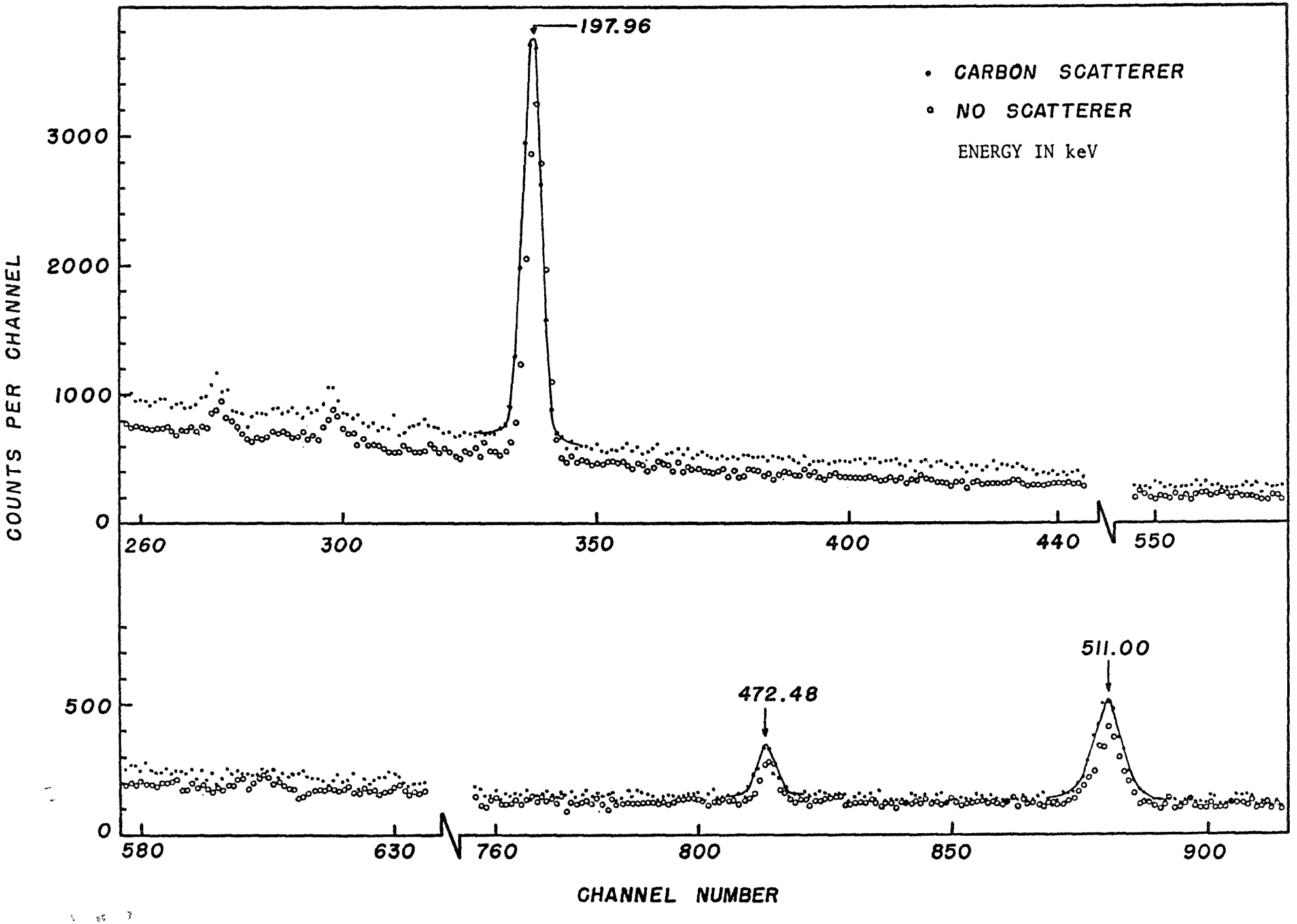
197.96
CARBON SCATTERER
NO SCATTERER
ENERGY IN keV
3000
2000
1000
0
COUNTS PER CHANNEL
260
300
350
400
440
550
511.00
472.48
500
0
580
630
760
800
850
900
CHANNEL NUMBER